ISSN 0016-7932, Geomagnetism and Aeronomy, 2007, Vol. 47, No. 3, pp. 285–290. © Pleiades Publishing, Ltd., 2007.
Original Russian Text © A.B. Askerov, V.N. Obridko, 2007, published in Geomagnetizm i Aeronomiya, 2007, Vol. 47, No. 3, pp. 303–308.

Magnetic Cloud in the Solar Wind: A Comparison with the Classical Model

A. B. Askerov[a] and V. N. Obridko[b]

[a] *Shemakha Astrophysical Observatory, Academy of Sciences of Azerbaijan, Shemakha, 373243 Azerbaijan*

[b] *Pushkov Institute of Terrestrial Magnetism, Ionosphere, and Radiowave Propagation, Russian Academy of Sciences, Troitsk, Moscow oblast, 142190 Russia*

Received March 20, 2006; in final form, November 1, 2006

Abstract—The solar wind magnetic field distribution near the Earth has been studied and compared with the distribution anticipated according to the classical model. It has been indicated that a two-hump distribution of the IMF values discovered previously is not an artifact of averaging but reflects the actual structure of the magnetic field within the sector. In this case the magnetic field of polarity corresponding to the leading spot in the Northern Hemisphere is encountered more frequently. Not only the magnetic field magnitude but also the fields of either polarity increase with increasing activity. The distance between the peaks on the histogram of the magnetic field near the Earth increases from 6 to 10 nT. The quasi-22-year, 11-year, and quasibiennial (2.6 ± 0.3 years) cycles are observed in an alternate increase in the peaks, in the strength of the fields of either polarity, and in the ratio of the peaks to the occurrence frequency of zero values, respectively. The classical model is violated in approximately 25% of cases.

PACS numbers: 96.50.Bh

DOI: 10.1134/S0016793207030024

1. INTRODUCTION

A popular concept of a quiet solar wind uses in its calculations a rather simple scheme of the source surface [Parker, 1958], which will subsequently be called a classical scheme for short. According to this scheme, the entire heliosphere is divided into two regions: the zones of a free field and the solar wind. In the first zone, the magnetic field exists as if in vacuum and completely depends on the observed field structure on the surface of the photosphere. The only additional condition consists in that the potential is zero and field lines are strictly radial somewhere on a conditional source surface. Farther in the interplanetary medium, the radial expansion takes place, and the field is completely carried away by the solar wind. Strictly speaking, under such assumptions, there are no fundamental difficulties in calculating the field near the Earth. The main difficulties are reduced to a correct measurement of the magnetic field at the level of the photosphere, introduction of corresponding corrections, and optimal selection of a source surface. In the main version [Hoeksema and Scherrer, 1986], it is assumed that the source surface is a sphere with a radius equal to 2.5 solar radii. On the average, the radial solar magnetic field in the interplanetary space should decrease as r^{-2} for a quiet outflow.

On the whole, the results proved to be very encouraging: the sign of B_{XE}—the IMF radial component near the Earth—was generally in good agreement with the sigh of B_{SS}, the radial component of the magnetic field on the source surface (taking into account a transport time of 4 days). The general calculated structure of the magnetic field is in rather good agreement with the observed structure [Obridko et al., 1994], apparently, because the structure generally depends on the large-scale solar field. This leads to another important conclusion for our problem: the first harmonics, responsible for the large-scale field, are calculated rather exactly. As a result, we can assume that the magnetic field on the source surface, characterized by several first harmonics, is calculated quite reliably. This means that the general structure of the magnetic field in the solar corona and in the near-Earth space should be calculated sufficiently adequately. This is confirmed by the results of comparing with the structure and polarization of the corona [Badalyan et al., 1999, 2002; Sykora et al., 2002] and by the correlation comparisons with IMF [Hoeksema and Scherrer, 1986; Obridko and Shelting, 1999a, 1999b]. Numerous comparisons of the magnetic field calculations with cyclic variations of large-scale activity, coronal mass ejections [Ivanov et al., 1999; Ivanov and Obridko, 2001], structure and polarization of the corona, position of coronal holes in the regions of the open solar magnetic field [Obridko and Shelting, 1999a], magnetic field signs in the sector structure [Obridko and Shelting, 1999b], and geomagnetic disturbances [Obridko and Shelting, 1992] indicate that the calculation system, relying upon the potential approximation and the concept of a constant spherically symmetric source surface, is generally suitable for calculation of the field structure.

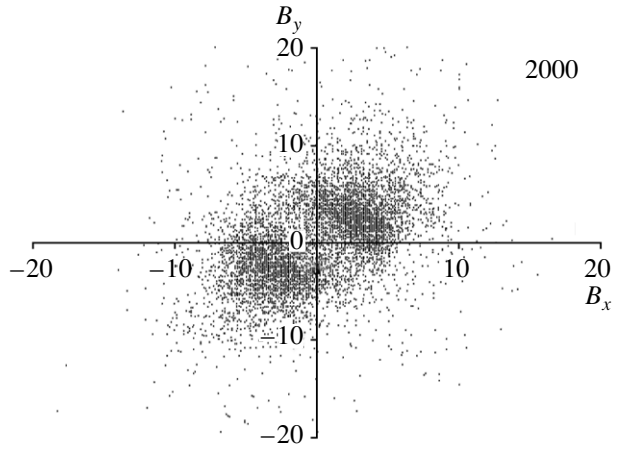

Fig. 1. The relationship of the measured average hourly values of B_X–B_Y for 2000.

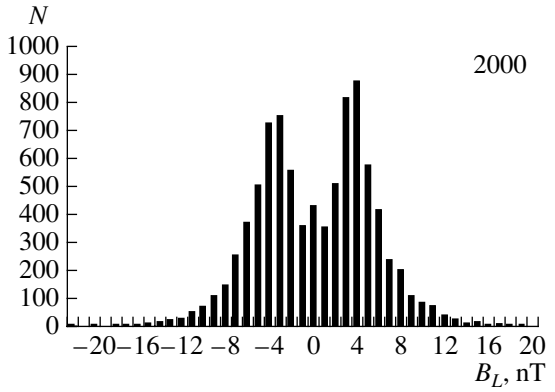

Fig. 2. The distribution of the B_L values for 2000.

However, the B_{XE} value, calculated based on the standard expansion law (r^{-2}), proved to be much smaller than the directly measured value [Obridko et al., 1996]. Obridko et al. [2004] tried to explain this difference by the introduction of the expansion law with an exponent slightly smaller than two. The attempts to improve the situation by changing the calculation scheme (the concept of a radial field in the photosphere, the transfer of the source surface at other altitude, and the introduction of two source surfaces) did not improve this situation fundamentally. The origin of a difference between the calculated field and the field measured in the heliosphere should be sought in different circumstances; therefore, one had to consider again the reliability of magnetic fields measured I the photosphere. In this case both IMF and variations in the galactic cosmic rays can be used as field value tests.

Obridko et al. [2006] analyzed all generally accepted calculation schemes and used initial data bases from the unified standpoint. It was indicated that these assumptions and limitations cannot distort the general structure and dependence on the cycle of solar and interplanetary data. At the same time, the values measured on the Sun are underestimated as a result of a magnetograph signal saturation. It was indicated that the correction should depend on both the heliocentric observation latitude and the solar cycle phase. The correction technique, which guarantees good agreement between calculated and measured values, was proposed. The created data base makes it possible to quantitatively calculate magnetic fields in the solar wind near the Earth.

Based on the daily data obtained by Obridko et al. [2006] for the prolonged period (1976–2004), Belov et al. [2006] subsequently calculated the solar magnetic field (B_S) at the geometric point of the Earth's projection on the solar wind source surface. These data were compared with the daily average values of the solar wind velocities and difference IMF components near the Earth. A statistical analysis revealed a sufficiently close relation between the solar wind characteristics near the Sun and the Earth during considerable sporadic solar and interplanetary disturbances. The numerical empirical models, which make it possible to calculate the solar wind velocity and IMF strength and longitudinal and B_z components based on solar magnetic field observations, were proposed. The B_S value plays the main role in all these models. It was indicated that variations in the *Ap* index of magnetic activity during quiet and relatively weakly disturbed periods can be predicted for three-five days ahead based on the solar magnetic field observations, and the quality of such a prediction is higher then that of the available predictions made using the traditional methods.

In this case the calculated values of the magnetic field on the source surface (B_S) were reduced to the values in the vicinity of the Earth (B_{XE}) using the r^{-2} law of radial expansion, as was done previously. According to this law, the distribution of the magnetic field values near the Earth should coincide with the distribution on the source surface to an accuracy of a constant scale factor.

However, the situation is slightly more complicated. On the one hand, The B_S sign correctly determines the IMF polarity in 84% of all days, and the correspondence of polarities is almost complete at sufficiently large $|B_S|$ values. At the same time, the relation between B_S and B_{XE} is evidently not linear, and polarities are often mixed at small $|B_S|$ values. It is evident that the values of the magnetic field strength close to zero are encountered much more often on the source surface than near the Earth. This fact becomes even more evident if we compare the distributions of the B_S and B_{XE} values (see Fig. 4 in [Belov et al., 2006]). The distribution of the field on the source surface is unimodal with the center of gravity at zero; however, the field distribution near the Earth is evidently bimodal with maximums near ±2.5 nT. A comparison of these distributions indicates that weak solar fields, as a rule, do not

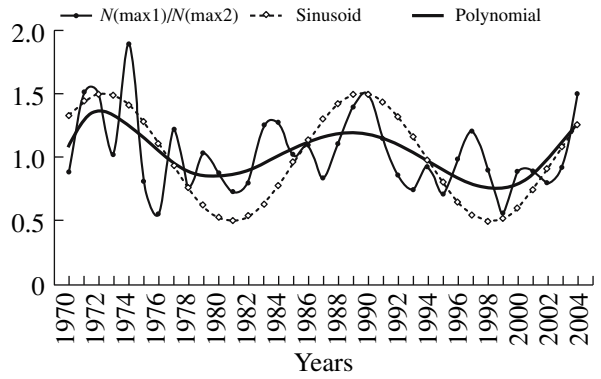

Fig. 3. The variations in the ratios of the histogram peak heights.

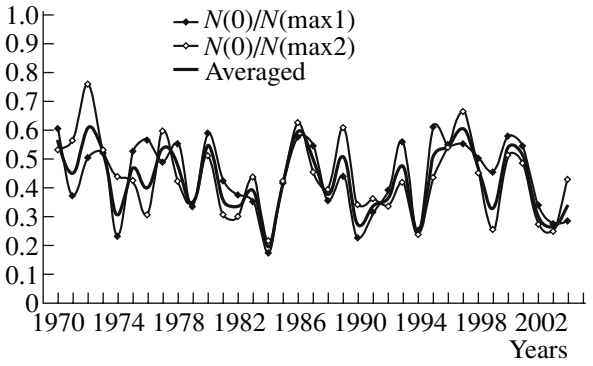

Fig. 4. The variations in the ratio of the histogram height, corresponding to zero B_L value, to the histogram peak height.

reach the Earth. This difference can partially be explained by the lower accuracy of determinations of the magnetic field on the source surface than the accuracy of interplanetary measurements; however, we assume that this difference is also caused by more serious physical factors. As was repeatedly mentioned [Obridko et al., 2004], the spherical surface of a source with a strictly radial magnetic field at all points is not more than abstraction. An actual magnetic field cannot be strictly radial over the entire sphere. This field expands below the source surface and (in certain regions, e.g., above coronal holes) does not remain radial above this surface too. In this process weak fields can be replaced by stronger ones, and the initial polarity remains not always.

The aim of this work is to thoroughly study this effect. Specifically, it was interesting to verify whether this effect is simply artifact of averaging and does not disappear when, e.g., average hourly values are used. If this effect actually exists, it would be interesting to examine how the characteristics of this effect depend on the time and phase of a solar cycle.

2. DIAGRAM OF THE RELATIONSHIP BETWEEN MEASURED AVERAGE H OURLY VALUES

The work uses the average hourly values of the solar wind velocity and the IMF characteristics from the OMNI data base (http://nssds.gsfs.nasa.gov/omniweb) for 35 years (1970–2004). Since the present work did not directly use the solar data, many limitations shown in [Obridko et al., 2004; Belov et al., 2006] are removed.

Figure 1 shows the diagram of the relationship between the measured average hourly values of B_x–B_y for 2000. It is clear that points are concentrated in the first and third quarters, which corresponds to the traditional model, taking into account the fact that the average velocity of the solar wind is close to the angular velocity of helix rotation. Nevertheless, rather many points are located in the second and fourth quarters, which is generally impossible within the scope of the Parker model at any propagation velocity. In principle, this is possible only under the assumption that a transversal component exists at the base of the solar wind, and this component can turn during propagation. These assumptions evidently contradict the classical model of a quiet solar wind but can be realized in nonstationary phenomena such as coronal mass ejections. Similar deviations from a simple spiral model were referred to by Veselovsky and Tarsina [2001]. The statistical properties of the solar wind and IMF parameters were also studied by Veselovsky et al. [2000, 2000b].

One more strangeness of Fig. 1 consists in that points where both field component are zero are almost absent, although vanishing of B_S should automatically make both IMF components vanish according to the classical concept.

In the absence of interplanetary interaction, within the scope of the classical model, the radial component of the B_S field near the Earth should be transformed into the field directed along the helical field line at an angle of $\psi = \arctan(\Omega R_E/V_{SW}$ with respect to the radius, where Ω is the Sun's rotational speed, R_E is the average distance from the Earth to the Sun, and V_{SW} is the solar wind velocity near the Earth. Let us calculate the IMF projection near the Earth onto the field line anticipated according to the V_{SW} value: $B_L = B_{XE}\cos(\psi) + B_{YE}\sin(\psi)$, ($B_{XE}$ and B_{YE} are the field components in the ecliptic plane). We will call this projection the longitudinal component of IMF. In the last expression, the signs of the B_{XE} component were selected so that the direction from the Sun should correspond to positive B_L values.

The distribution of the B_L values for 2000, calculated in such a way, is shown in Fig. 2. It is clear that the B_L distribution remained bimodal after the usage of the average hourly values. Moreover, the histogram became wider, and the values of the maximums (peaks) on the diagram of the average hourly values correspond

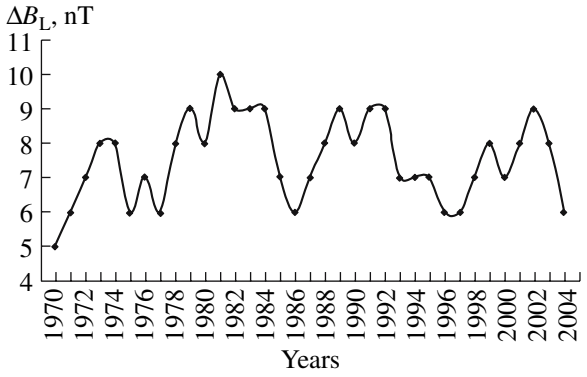

Fig. 5. The time variations in the distance between the peaks (ΔB_L).

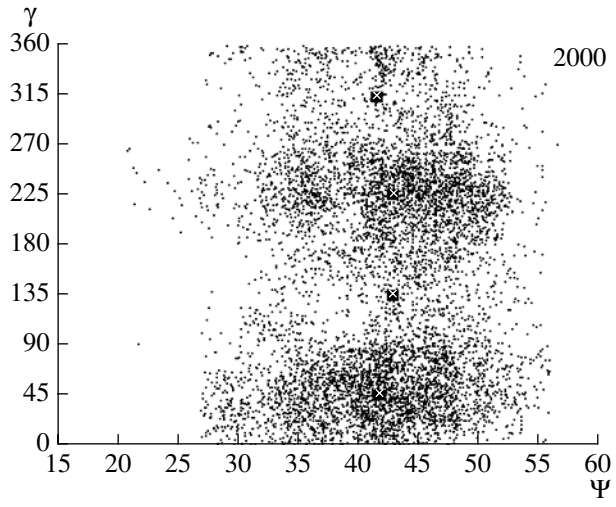

Fig. 6. Diagram of angles ψ–γ for 2000.

to ±4.5 nT. It is important to note that the heights of these maximums (max1 and max2) are different, and the ratio of these heights varies in time.

To consider the dynamics of the B_L peaks, we constricted the pattern of variations in these peaks relative to one another and relative to the zero value. The variations in the N(max1)/N(max2) ratio is shown in Fig. 3, which also demonstrates the approximating polynomial of the sixth degree (black solid line) and the sinusoid with a period of ~17.25 years (dotted line). It is evident that, within the scope of a limited realization, a period of ~17 years is statistically indistinguishable from 30 years, which has been the main Hale cycle for the last years.

It is evident that the maximal deviations from the peak equality (i.e., from unity) correspond to the Wolf number maximums, and the passage through unity corresponds to the phases of solar cycle minimums. It is important to note that the periodicity in Fig. 3 is close to 20 years; this means that the sign of a local field (i.e., the Hale law) participates in the formation of bimodality. Indeed, taking into account the Hale law, we can state that fields with the direction coinciding with the direction of the field in the leading spot in the groups of the Northern Hemisphere have been encountered more frequently in the interplanetary medium for the last 35 years. In 1971 and 1990 (cycles 20 and 22), this ratio was larger than 1; i.e., max1(corr. $-B_L$) > max2(corr. $+B_L$). In 1980 and 1998 (cycles 21 and 23), this ratio was smaller than 1; i.e., max1(corr. $-B_L$) < max2(corr. $+B_L$).

We have not seen any significant regularity, except the well-known quasibiennial variations with a period of 2.6 ± 0.3 year, in the ratio of the histogram height (corresponding to zero B_L value) to the peak heights (see Fig. 4).

Figure 5 demonstrates the time variations in the distance between the peaks (ΔB_L). A rather distinct regularity is observed here: the peaks diverge up to 9–10 nT during the periods of maximums and converge to 6 nT during the periods of minimums. All four cycles are identical in this respect independently of the signs of the global and local solar fields.

3. COMPARISON OF THE SOLAR WIND AND MAGNETIC FIELD DIRECTIONS

Since independent observations give the solar wind velocity (V_{SW}) and the B_X and B_Y components of the magnetic field, we can calculate the direction of the solar wind (plasma angle ψ) and magnetic field line γ if the average velocity of Sun's rotation is known: $\psi = \arctan(\Omega R_E/V_{SW})$, and $\gamma' = \arctan(B_X/B_Y)$. In this case:

(a) if $B_X > 0$ and $B_Y > 0$, $\gamma = \gamma'$; i.e., angle γ is within 0°–90°;

(b) if $B_X < 0$ and $B_Y > 0$, $\gamma = 90 - \gamma'$; i.e., angle γ is within 90°–180°;

(c) if $B_X < 0$ and $B_Y < 0$, $\gamma = 180 + \gamma'$; i.e., angle γ is within 180°–270°;

(d) if $B_X > 0$ and $B_Y < 0$, $\gamma = 360 + \gamma'$; i.e., angle γ is within 270°–360°.

Similar conditions were introduced for angle ψ.

In the Parker theory, these angles are assumed to be identical by definition. Indeed, these angles are rather close to each other (see Fig. 6). However, many points fall in quadrants 2 and 4, which does not correspond to the classical theory. Filled squares are the centers of gravity of the corresponding intervals: 0°–90°, 90°–180°, 180°–270°, and 270°–360°; 42° on average.

The closeness of these angles also remains for their average annual values. Thus, the observed points are divided into two families. The majority of the points fall in quadrants 1 and 3, and their statistics is in good agreement with the classical theory. However, a rather large number of the points (about 25%) do not fall in quadrants 1 and 3 and, thus, disagree with the classical

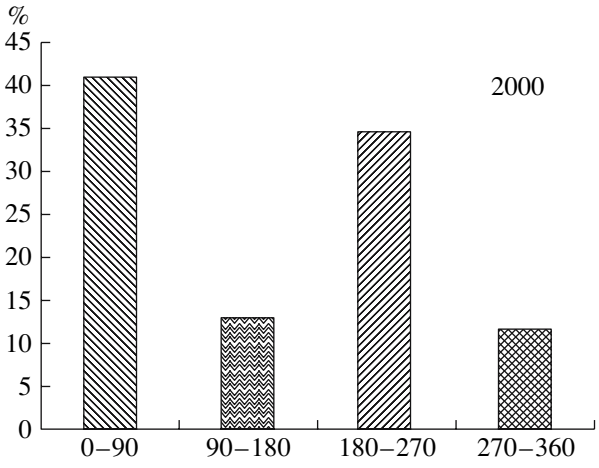

Fig. 7. The relative number of points in quadrants 1–4 for 2000.

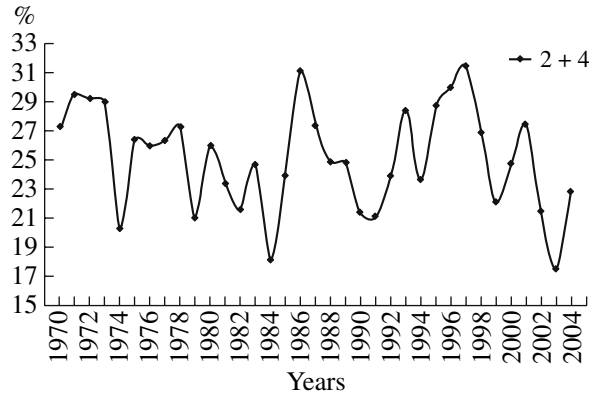

Fig. 8. The time variations in the relative number of points in quadrants 2 and 4 (in %).

theory. The relative number of the points (in percent) in quadrants 1–4 for 200 is shown in Fig. 7.

The statistics of the distribution of these angles (in %) for 2000 is as follows:

	$-B_X$	B_X
B_Y	13.1%	40.9%
$-B_Y$	34.4%	11.6%

The relative number of the points in quadrants 2 and 4 (in percent of the total number in a year) is shown in Fig. 8. We could anticipate that the number of these points would be maximal during the periods of high activity, when mass ejections strongly disturb a quiet solar wind. However, this is not the case, and any distinct periodicity is not observed in these data.

4. CONCLUSIONS

We indicated that a bimodal distribution of the IMF values is not an artifact of averaging but reflects an actual pattern of the magnetic field within a sector. In this case the magnetic field, the polarity of which corresponds to that of a spot in the Northern Hemisphere, is encountered more frequently.

Not only the magnetic field magnitude but also the individual fields of either polarity increase with increasing activity. The distance between the peaks increases from 6 to 10 nT.

The quasi-22-year, 11-year, and quasibiennial cycles are observed in the alternate increase in the peaks, the strength of the fields of either polarity, and the ratio of the peaks to the occurrence frequency of zero values, respectively.

The classical model is violated in approximately 25% of cases.

ACKNOWLEDGMENTS

This work was supported by the Russian Foundation for Basic Research, projects nos. 04-02-16763, 05-02-16090, and 05-02-17251.

REFERENCES

1. O. G. Badalyan, V. N. Obridko, and J. Sykora, "Polarization in the 530.3 nm Emission Line and Coronal Magnetic Field Structure," Contrib. Astron. Obs. Skalnate Pleso **32**, 175–189 (2002).
2. O. G. Badalyan, V. N. Obridko, and Yu. Sykora, "Relation between the Green-Line Polarization of the Solar Corona and Coronal Magnetic Fields," Astron. Zh. **76** (11), 869–880 (1999) [Astron. Rep. **43** (11), 767 (1999)].
3. A. V. Belov, V. N. Obridko, and B. D. Shelting, "Correlation between the Near-Earth Solar Wind Parameters and the Source Surface Magnetic Field," Geomagn. Aeron. **46** (4), 456–464 (2006) [Geomagn. Aeron. **46**, 430–437 (2006)].
4. L. Biermann, "Solar Corpuscular Variation and the Interplanetary Gas," Observatory **77**, 109–110 (1957).
5. J. T. Hoeksema and P. H. Scherrer, *The Solar Magnetic Field-1976-through1985, UAG Report, 94* (WDC-A for Solar Terrestrial Physics, 1986).
6. E. V. Ivanov and V. N. Obridko, "The Cyclic Variations of the CME Velocity," Sol. Phys. **19**, 179–196 (2001).
7. E. V. Ivanov, V. N. Obridko, E. V. Nepomnyashchaya, and N. V. Kutilina, "Relevance of CME to the Structure of Large-Scale Solar Magnetic Fields," Sol. Phys. **184**, 369–384 (1999).
8. V. N. Obridko and B. D. Shelting, "Cyclic Variation of the Global Magnetic Field Indices," Sol. Phys. **137** (1), 167–177 (1992).
9. V. N. Obridko and B. D. Shelting, "Structure and Cyclic Variations of Open Magnetic Fields," Sol. Phys. **187**, 185–205 (1999a).
10. V. N. Obridko and B. D. Shelting, "Structure of the Heliospheric Current Sheet as Considered over a Long Time Interval (1915–1996)," Sol. Phys. **184**, 187–200 (1999b).

11. V. N. Obridko, A. F. Kharshiladze, and B. D. Shelting, "Certain Methodical Problems of Calculations of Harmonic Coefficients of Global Magnetic Fields," in *Solar Magnetic Fields and Helioseismology* (FTI, St. Petersburg, 1994), pp. 71–80 [in Russian].

12. V. N. Obridko, A. F. Kharshiladze, and B. D. Shelting, "On Calculating the Solar Wind Parameters from the Solar Magnetic Field Data," Astron. Astrophys. Trans. **11**, 65–79 (1996).

13. V. N. Obridko, B. D. Shelting, and A. F. Kharshiladze, "Multivariate Calculations of the Solar Wind Parameters from the Data on the Solar Magnetic Field," Astron. Vestn. **38** (3), 261–272 (2004).

14. V. N. Obridko, B. D. Shelting, and A. F. Kharshiladze, "Calculation of the Interplanetary Magnetic Field Based on Its Value in the Solar Photosphere," Geomagn. Aeron. **46** (3), 310–319 (2006) [Geomagn. Aeron. **46**, 294–302 (2006)].

15. E. N. Parker, "Dynamics of the Interplanetary Gas and Magnetic Fields," Astrophys. J. **128**, 664–676 (1958).

16. J. Sykora, O. G. Badalyan, and V. N. Obridko, "Relationship between the Coronal Shape and the Magnetic Field Topology during the Solar Cycle," Adv. Space Res. **29**, 395–400 (2002).

17. I. S. Veselovsky and M. V. Tarsina, "Angular Distribution of the Interplanetary Magnetic Field Vector," Geomagn. Aeron. **41** (4), 471–476 (2001) [Geomagn. Aeron. **41**, 452–456 (2001)].

18. I. S. Veselovsky, A. V. Dmitriev, A. V. Suvorova, and Yu. S. Minaeva, "Structure of Long-Term Variations in the Parameters of the Plasma and Magnetic Field in the near-Earth Heliosphere," Astron. Vestn. **34**, 82–93 (2000a).

19. I. S. Veselovsky, A. V. Dmitriev, Yu. V. Orlov, et al., "Modeling of the Statistical Spatial Distributions of the Solar Wind and IMF Using the Artificial Neural Networks," Astron. Vestn. **34**, 131–138 (2000).